L-shell ionization of Si, P, S, Cl, and Ar by 0.4- to 2.0-MeV H^+ and 0.4- to 1.2-MeV H_2^+ bombardment

W. M. Ariyasinghe, H. T. Awuku, and D. Powers
Department of Phyics, Baylor University, Waco, Texas 76798
(Received 30 May 1990)

L-shell-ionization cross sections of Si, P, S, Cl, and Ar have been obtained for incident H^+ energies of 0.4 to 2.0 MeV and for H_2^+ energies of 0.4 to 1.2 MeV. These relative cross sections were obtained from Auger-electron yields measured from gaseous targets of SiH_4, PH_3, SO_2, CH_3Cl, and Ar. The normalized experimental L-shell-ionization cross sections are compared to existing experimental L-shell-ionization cross sections and to various theoretical predictions.

I. INTRODUCTION

Brandt and Lapicki[1] in 1979 indicated a need for experimental L-shell-ionization cross-section measurements for third-row elements because the few measurements in S and Cl disagree with the existing theories. In a recent paper[2] we reported experimental L-shell-ionization cross sections for the third-row elements Si, P, S, Cl, and Ar under 0.4- to 2.1-MeV He^+ ion bombardment of elemental Ar and gaseous compounds of the other four elements. These cross sections were obtained from measured Auger-electron yields following L-shell-ionization of the target atoms, and were compared with the energy-loss Coulomb-deflection perturbed stationary-state relativistic (EPSSR), relativistic plane-wave Born approximation (PWBAR), and binary-encounter approximation (BEA) predictions as well as to existing experimental L-shell-ionization cross sections of Cl and Ar.[3-5] The Ar L-shell-ionization cross sections agreed within the 12% experimental random error to the ECPSSR prediction and to experimental cross sections produced elsewhere. The Cl L-shell-ionization cross sections were found to be 2.5 times lower than the measurements of Maeda *et al.*,[5] but were below the ECPSSR theory by 40% and below the PWBAR theory by 30% at He^+ ion energies >1.2 MeV. The S and Si L-shell-ionization cross sections produced in this laboratory were 34–62% below the ECPSSR and PWBAR theories for all He^+ ion energies, while the P cross sections were below the same theories by 33–45% at higher He^+ ion bombarding energies. All experimental L-shell-ionization cross sections produced in this laboratory fell below the BEA theory from 17% to 64%. No other L-shell measurements exist for Si, P, and S under He^+ ion bombardment at these energies.

The present paper extends the He^+ measurements in Ref. 2 to the same third-row elements Si, P, S, Cl, and Ar using the same experimental technique and the gaseous substances SiH_4 (silane), PH_3 (phosphine), SO_2 (sulfur dioxide—replaces the hydrogen sulfide used in the former experiment), CH_3Cl (methyl chloride), and Ar, but employing instead 0.4- to 2.0-MeV H^+ ions and 0.4- to 1.2-MeV H_2^+ ions. No prior L-shell-ionization cross-section measurements exist for Si and P under H^+ or H_2^+ bombardment, but several measurements exist for S, Cl, and Ar.[3-7] The present measurements are compared with the existing experimental measurements and to the same theoretical predictions ECPSSR, PWBAR, and BEA.

II. EXPERIMENT

A detailed description of the experimental method is given in Ref. 2. Briefly, 0.4- to 2.0-MeV H^+ ions and 0.4- to 1.2-MeV H_2^+ ions from a Van de Graaff accelerator were magnetically analyzed and directed into an 18-in.-diam scattering chamber shielded with mu metal and pumped by a Leybold-Heraeus Model TMP turbomolecular pump to the low 10^{-6} Torr region. The scattering chamber contained an electron trap to remove secondary electrons, a 6-cm-long rectangular-shaped differentially-pumped gas cell with open end windows, and a Faraday cup to collect the ion current. The entrance and exit apertures of the gas cell were 1.0 and 1.2 mm diam, respectively. Research-grade target gases of Ar, CH_3Cl, SO_2, and SiH_4 from Matheson Co., Laporte, Texas, and PH_3 from Liquid Air Corp., Denver, Colorado, all with minimum purities of 99.5% or better, were directed through a gas transport system into the gas cell at equilibrium pressures of 3 mTorr measured by a calibrated Varian Model 531 Thermocouple Gauge. Target gas purities were confirmed by an Ametek Residual Gas Analyzer, Model MA 100, which also was used to guarantee no air leak or other gas contamination into the system. The Auger electrons exited the gas cell through a 1-mm-diam hole at 90° to the incident ion beam direction and entered a 160° spherical sector electrostatic analyzer (ESA) from Comstock, Inc., Oak Ridge, Tennessee, operated in constant 30-eV transmission mode with 0.45-eV resolution or better. At the exit port of the ESA was a microchannel plate detector with two microchannel plates, Model VUW-8960ES, from Varian Associates, Palo Alto, California, positioned in chevron configuration.

In the present experiment, the method of data collection is identical to that in Ref. 2. The retarding ramp voltages were the same as those used in the previous experiment, and are -35 to -145 V (Si), -45 to -155 V(P), -65 to -175 V (S), -90 to -200 V (Cl), and -120 to -230 V (Ar). These voltages were applied to

the ESA to acquire the Auger spectra, which were collected in an EG&G Ortec Model 7150 Multichannel Analyzer (MCA). These ramp voltages were selected to ensure that each Auger spectrum was collected in the middle portion of the MCA viewing screen with sufficient overlap at the low- and high-energy portions of the spectrum to allow for meaningful background subtraction. The total charge collected in the Faraday cup for each spectrum was 4.10×10^{-4} C of H^+ (or H_2^+), which was the same as for He^+ in the previous experiment.

The microchannel plate (MCP) efficiency corrections and the ESA transmission efficiency corrections were identical to those in Ref. 2. The MCP efficiency corrections were made relative to the efficiency for Ar Auger electrons, and were 30% (Si), 17% (P), 8% (S), and 3% (Cl) with corresponding error assignments to Auger *LMM* Auger yields of 9% (Si), 5% (P), and 3% (S and Cl). The ESA transmission efficiency corrections were 81% (Si), 37% (P), 18% (S), 6.3% (Cl), and 0% for Ar with respective random error assigned to the corrections of 15% (Si), 8.5% (P), 4.0% (S), 1.5% (Cl), and 0% (Ar). It is important to state that the ESA transmission efficiencies were found to be the same using either He^+ or H^+ ions. Since the ESA transmission properties refer to the transmitted Auger electrons themselves, no difference would be expected when H_2^+ ions produce the electrons.

Typical ion beam currents of H^+ and H_2^+ were 100 nA. When a 0 to +245 V bias was applied to the Faraday cup there was no change in the H^+ ion beam current. The H^+ (or H_2^+) ion beam current was measured at 0.2-MeV intervals from 0.4 to 2.0 MeV (0.4–1.2 MeV for H_2^+) with and without each of the target gases in the cell at 3 mTorr pressure. The H^+ ion current was found to be the same ($\sim$100 nA) with or without the target gas in the cell for all five gases. In contrast, the same measurements with the H_2^+ ion beam revealed the current to increase in the presence of the four gases SiH_4, PH_3, CH_3Cl, and Ar by 50% with a random error or 4%. When the gas cell was filled with SO_2 at 3 mTorr pressure, however, the increase of the H_2^+ ion beam current was 60% with a 5% random variation. It is well known that when energetic ions pass through matter, they lose and/or capture electrons in collisions with atoms of the materials through which they pass.[8,9] It is seen from Ref. 8 that the electron-loss probability is 97% or greater for 0.2 MeV or higher energy proton beams, while electron capture probability becomes dominant only for proton beams below 15 keV. Since the H^+ ion energies in this work are greater than 0.2 MeV, no electron capture or loss will occur when the H^+ beam passes through the gas cell.

When a molecular H_2^+ beam of energy $\geq$0.4 MeV passes through the gas cell, however, there is no electron capture, because the lowest energy of 0.4 MeV is equivalent to a 0.2-MeV H^+ beam. There is a high probability that the electron in H_2^+ will be stripped from the ion by the target gas. If all the electrons in the H_2^+ ion beam are lost, two protons will be left and the current at the Faraday cup will increase by a factor of 2. The observed current increase from 50% to 60% at 3 mTorr pressure, and to 80% at 6 mTorr pressure, however, demonstrate that charge equilibrium has not been obtained. The same 4.10×10^{-4} C of charge was used from the H_2^+ ion beam as from the H^+ beam to obtain the Auger cross sections.

In order to test for incomplete transmission of H^+ (or H_2^+) ions through the gas cell, the beam current was measured with and without the back plate of the gas cell when no gas was in the cell. This measurement revealed that only 3% of the beam was lost inside the gas cell. When the same measurement was made with Ar gas at 3 mTorr pressure, a 4% current loss occurred. This loss was taken into account in the determination of the Auger cross sections.

The same procedure used in the previous experiment[2] was employed to ensure that the MCP efficiency and ESA transmission efficiency had not changed throughout the course of the experiment, namely, to measure the Ar *LMM* Auger yield per incident H^+ (or H_2^+) ion per target atom before and after *LMM* Auger yields had been obtained at all energies from each of the other target gases. A range of variation in the Ar Auger yield was found to be from -5% to $+5\%$ for H^+, and from -1% to $+6\%$ for H_2^+ of the Ar values given in this paper. It should also be mentioned that the all measurements were repeated once at all H^+ (or H_2^+) energies.

The relative errors in this experiment are found to be essentially the same as in the previous experiment[2] except for the error in the background subtraction. In this experiment, the estimated errors in the background subtraction are 10% for Si, P, Cl, and Ar. The error for S is found to be 16%, which is about 6% greater than in the previous experiment for S. This larger uncertainty was caused by the use of SO_2 in this experiment instead of H_2S in the other experiment. Other random errors in the present experiment are gas-pressure measurements (error $\leq$5%), atmospheric contamination of target gas (error $\leq$1%), beam current measurements (error $\leq$5%), MCP efficiency calibration (error of 1–9%), and ESA transmission efficiency calibration (error of 0–15%). These random errors and the error in the background subtraction combine quadratically to give a maximum random error assignment of 22% (Si), 16% (P), 17% (S), and 12% (Cl and Ar), which are essentially the same as the errors given in Ref. 2, except for S which is 4% greater than in the previous work.

Finally, all *LMM* Auger electron yields were normalized to the Ar yield which in turn was normalized to Stolterfoht's value[3] for Ar for 0.6-MeV H^+, to which he assigned an 18% error. Thus, our relative error of 12–22% will be combined together with Stolterfoht's error assignment of 18%.

III. RESULTS

Typical $L_{23}MM$ Auger-electron spectra of Si, P, S, Cl, and Ar produced by 1.0-MeV H^+ ion bombardment of SiH_4, PH_3, SO_2, CH_3Cl, and Ar, respectively, are given in Fig. 1. These spectra are superimposed on the secondary electron spectra, which are subtracted by the procedure

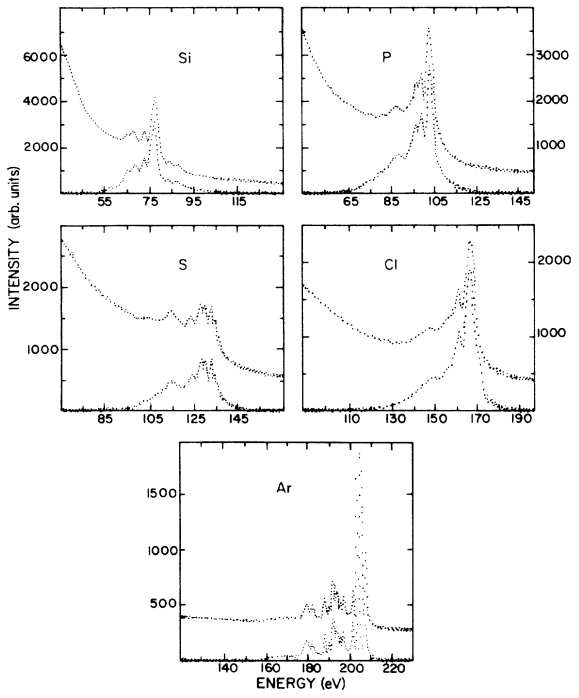

FIG. 1. *LMM* Auger-electron spectra of Si, P, S, Cl, and Ar as a function of energy in eV. The spectra are produced by 1.0-MeV H^+ ion bombardment of SiH_4, PH_3, SO_2, CH_3Cl, and Ar, respectively. The top curve is the spectrum including the background, while the lower curve gives the Auger spectrum after the background has been subtracted. The vertical scale in each case represents the number of Auger electrons recorded in arbitrary units.

given in Ref. 1, namely, by curve fitting the lower and upper energy ends of the background spectra by a suitable polynomial fit. Third-degree polynomials are used for SiH_4, PH_3, and SO_2, second-degree polynomials for Ar, and either second- or third-degree polynomials for the CH_3Cl background spectra for all H^+ or $H_2{}^+$ bombarding energies. The background spectra for SiH_4 and PH_3 under H^+ and $H_2{}^+$ bombardment are found to decrease less noticeably with increasing electron energy than similar spectra produced in Ref. 2 by He^+ ion bombardment. Each Auger spectrum in Fig. 1, represented by the lower graph, is obtained by subtracting the curve-fitted background from the upper graph which represents the combined Auger-plus-background spectrum.

The Auger spectra after background subtraction were integrated to obtain Auger-electron yields which were then converted to Auger cross sections relative to that of Ar at 0.6-MeV H^+ by Stolterfoht *et al.*[3] In these cross-section calculations, it is assumed that the Auger-electron emission is isotropic as it is assumed by several other authors[3,4,7,10] and by us[2,11,12] previously. The reported anisotropy in *LMM* Auger emission by Cleff and Melhorn[13] is about 10%, which is smaller than the experimental errors of 12–22% in this experiment, but would lower our experimental values systematically.

It has been shown in detail in Ref. 2 that the total Auger cross sections obtained in this experiment are essentially the total L-shell-ionization cross sections.[2] L-shell-ionized atoms undergo Auger transitions, Coster-Kronig transitions, and radiative (x-ray) transitions. In Si, P, S, Cl, and Ar, Coster-Kronig transitions convert most of the L_1 vacancies into L_2 or L_3 vacancies,[14] since a L_1 vacancy is immediately filled with an electron from either the L_2 or L_3 shell. The radiative transition yields (fluorescence yields) are negligible for the series of atoms in this study,[14] so the $L_{23}MM$ Auger process is the dominant mechanism for filling the ionized L-shell vacancies.

The experimental L-shell-ionization cross sections for Si, P, S, Cl, and Ar are given in Tables I and II, respectively, for 0.4- to 2.0-MeV H^+ and for 0.4- to 1.2-MeV $H_2{}^+$. The errors are probable random errors as discussed in Sec. II. The gaps in the tables are caused by experimental difficulty in collecting the spectra due to excessive electronic noise and the occasional appearance of elastically scattered electrons that have the same velocity as the ion bean in some instances which makes the background subtraction process untenable. The cross sections given in Table II are divided by 2 to allow for a comparison of cross sections per incident charged nucleus. The variation of L-shell-ionization cross section as a function of projectile energy per amu is given in Figs. 2–6 for Si, P, S, Cl, and Ar, respectively. The solid circles represent

TABLE I. L-shell-ionization cross sections of Si, P, S, Cl, and Ar produced, respectively, by H^+ bombardment of SiH_4, PH_3, SO_2, CH_3Cl, and Ar gases. The errors are probable random errors.

H^+ ion energy (MeV)	E/A (MeV/amu)	Si cross section (10^{-17} cm^2)	P cross section (10^{-17} cm^2)	S cross section (10^{-17} cm^2)	Cl cross section (10^{-17} cm^2)	Ar cross section (10^{-17} cm^2)
0.4	0.4					0.33±0.04
0.5	0.5	1.53±0.33	1.17±0.20	0.77±0.13		0.38±0.04
0.6	0.6	1.43±0.31	1.18±0.16	0.75±0.13	0.51±0.06	0.38±0.04
0.8	0.8	1.34±0.30	0.97±0.15	0.69±0.12	0.53±0.07	0.38±0.04
1.0	1.0	1.28±0.28	0.84±0.13	0.59±0.10	0.52±0.06	0.37±0.04
1.2	1.2	0.99±0.22	0.73±0.13	0.57±0.07	0.53±0.06	0.33±0.03
1.4	1.4	1.06±0.23	0.73±0.10	0.49±0.05	0.50±0.06	0.29±0.03
1.6	1.6	0.94±0.21	0.68±0.09	0.45±0.06	0.46±0.05	0.27±0.02
1.8	1.8	0.91±0.20	0.62±0.10	0.43±0.05	0.45±0.05	0.26±0.02
2.0	2.0	0.72±0.15	0.56±0.08	0.38±0.06	0.41±0.05	

TABLE II. L-shell-ionization cross sections of Si, P, S, Cl, and Ar produced, respectively, by H_2^+ bombardment of SiH_4, PH_3, SO_2, CH_3Cl, and Ar gases. These cross sections are divided by 2 to represent the cross section per incident charged nucleus. The errors are probable random errors.

H_2^+ ion energy (MeV)	E/A (MeV/amu)	Si cross section (10^{-17} cm^2)	P cross section (10^{-17} cm^2)	S cross section (10^{-17} cm^2)	Cl cross section (10^{-17} cm^2)	Ar cross section (10^{-17} cm^2)
0.4	0.20	2.09±0.43	1.31±0.21			
0.5	0.25	2.31±0.46	1.30±0.20	0.60±0.10	0.43±0.05	
0.6	0.30	2.04±0.44	1.28±0.20	0.65±0.11	0.46±0.06	
0.8	0.40	1.96±0.42	1.35±0.21	0.70±0.12	0.58±0.07	0.37±0.04
1.0	0.50	1.80±0.40	1.30±0.21	0.65±0.10	0.59±0.07	0.38±0.04
1.2	0.60	1.70±0.36	1.23±0.19		0.59±0.07	0.39±0.04

proton measurements at higher energies and × represents H_2^+ measurements at lower energies; the two sets of measurements join nicely. ECPSSR and PWBAR theoretical L-shell-ionization cross sections from $E/A=0.1$ to 1.2 MeV/amu by Lapicki[15] are given on each figure, and experimental cross sections for S, Cl, and Ar produced at other laboratories are also included for comparison. The dotted portions on the theoretical curves from $E/A=1.2$ to 2.0 MeV/amu are our own logarithmic derivative extensions of Lapicki's curves.

An examination of target-atom Z_2 dependence of L-shell-ionization cross sections is given in Fig. 7, where the experimental cross sections are scaled according to the BEA universal curve[16] $U_L^2\sigma_L/Z_1^2$ as a function of $E/(\lambda U_L)$, where U_L is the binding energy of the L-shell electron (we used the values given by de Alti and Decleva[17]), σ_L is the L-shell-ionization cross section, Z_1 is the atomic number of the projectile, E is the energy of the projectile, and λ is the ratio of H^+ mass-to-electron mass. The solid curve given in the figure is the BEA theoretical prediction given by Hansen.[16]

In Fig. 8 is plotted the ratio of $\sigma(He^+)/4\sigma(H^+)$ or $\sigma(He^+)/4\sigma(H_2^+)$ as a function of ion energy in MeV/amu to examine the projectile Z_1^2 dependence. The experimental $\sigma(He^+)$ values are given in Ref. 2. The theoretical predictions of Lapicki[15] along with measurements[3–5] obtained in other laboratories are included for comparison.

IV. DISCUSSION

For the five elements Si, P, S, Cl, and Ar, the PWBAR theoretical L-shell-ionization cross-section predictions are lower than those of the ECPSSR theory by less than 12% for H^+ and H_2^+ ions of energy per amu of 0.2 to 1.2 MeV/amu (and of our extrapolation of the theories from 1.2 to 2.0 MeV/amu), but may exceed this 12% outside this region. Since this 12% difference is relatively small, we will, therefore, compare the experimental cross sections only with the ECPSSR theory in the discussion which follows.

In Fig. 2 it is seen that the experimental L-shell-ionization cross sections for Si are about 38% (at $E_{H^+}=2.0$ MeV) to 24% (at $E_{H^+}=1$ MeV) below the ECPSSR theory. For all H_2^+ bombarding energies, within experimental errors, the experimental cross sections are in fair agreement with the ECPSSR theory. In Fig. 3 for $E_{H^+}<0.8$ MeV and for all H_2^+ bombarding energies the experimental cross sections for P are within 15% of the ECPSSR values. For proton energies above 1.0 MeV, however, the cross sections are about 26% below the ECPSSR theory. No prior experimental measurements for Si or P exist for H^+ or H_2^+ bombardment for comparison purposes.

It is seen in Fig. 4 that the experimental L-shell-ionization cross sections for S produced by bombardment of SO_2 by H^+ ions in this work and in Ref. 7 are in good agreement. Although the cross sections produced under

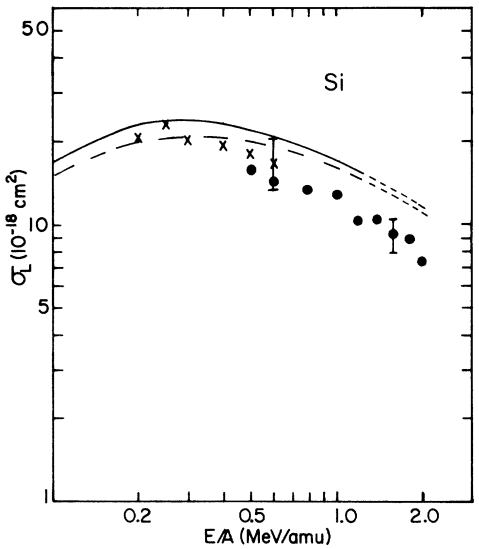

FIG. 2. L-shell-ionization cross sections in 10^{-18} cm^2 in Si for H^+ and H_2^+ ions in MeV/amu units. The solid and dashed curves are, respectively, the ECPSSR and PWBAR theories calculated by Lapicki (Ref. 15). The dotted curves from $E/A=1.2$–2.0 MeV/amu represent our logarithmic derivative extensions of Lapicki's theory. The closed circles are experimental cross sections of Si in SiH_4 for H^+ ions while the × are for H_2^+ ions.

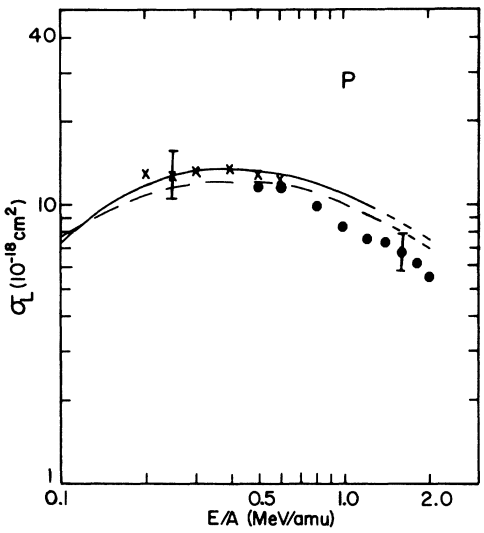

FIG. 3. Same as Fig. 2 for P; the experimental cross sections are for P in PH_3.

H^+ bombardment of SF_6 in Refs. 6 and 7 are in fair agreement with each other, they are 50% (for H_2^+ ions at 0.6 MeV) to 66% (for H^+ ions at 0.5 MeV) lower than the S measurements from SO_2 in this work. This difference in L-shell-ionization cross sections of S in different molecular environments was first pointed out and discussed by Matthews *et al.*,[7] who indicated the difference is caused by chemical effects in these different molecules. The S L-shell-ionization cross sections produced by bombardment of SO_2 by H^+ or by H_2^+ in this work and in Ref. 7 are 34% (at H^+ energy of 2.0 MeV) to 12% (at H^+ energy of 0.6 MeV) lower than the ECPSSR theory, while those produced by 0.8- to 1.0-MeV H_2^+ bombardment are about 23% below the theory.

In Fig. 5 the L-shell measurements of Maeda *et al.*[4] are about 10–73 % above the ECPSSR theory, while our measurements are in fair agreement with the theory but are 15–100% below Maeda's values. This other group used gaseous CCl_2F_2 for their target gas, and we have discussed in Ref. 2 that this compound has more electron screening and chemical-binding effects than in the CH_3Cl we used in our measurements.

In Fig. 6 the experimental Ar L-shell-ionization cross sections produced in this laboratory from $E/A=0.4$–1.8 MeV/amu are only about 5–15 % below the ECPSSR theory, but are 17% (at $E/A=0.8$ MeV/amu) to 80% (at $E/A=1.0$ MeV/amu) higher than the measurements of Maeda *et al.*[4] Within experimental errors, the Ar cross sections produced in this laboratory and those produced by Stolterfoht *et al.*[3] follow the general trend of the ECPSSR theory. The D^+-induced Ar L-shell-ionization cross sections of Watson and Toburen[5] are 18% below our relative measurement of 0.5 MeV/amu. It is to be pointed out that our relative cross-section measurements are all normalized to Stolterfoht's Ar value for 0.6-MeV H^+ ions.

In Fig. 7, where the experimental L-shell-ionization

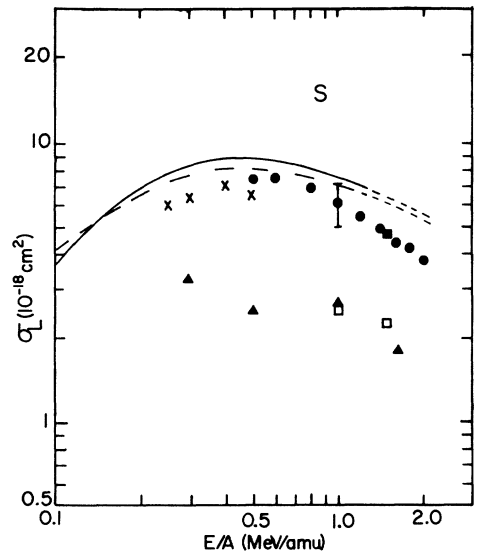

FIG. 4. L-shell-ionization cross sections in 10^{-18} cm^2 in S for H^+ and H_2^+ ions in MeV/amu units. The solid and dashed curves are, respectively, the ECPSSR and PWBAR theories calculated by Lapicki (Ref. 15) and the dotted curves are our extensions. The closed triangles and open squares, respectively, are experimental measurements by Toburen *et al.* (Ref. 6) and by Matthews and Hopkins (Ref. 7) for SF_6 under H^+ ion bombardment. The closed circles (H^+ bombardment) and × (H_2^+ bombardment) are the present experimental cross sections in SO_2 while the closed squares are cross sections produced by Matthews and Hopkins (Ref. 7) in SO_2 under H^+ ion bombardment.

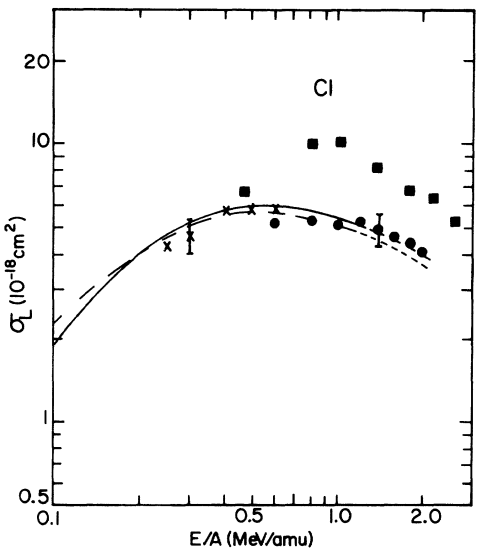

FIG. 5. L-shell-ionization cross sections in 10^{-18} cm^2 in Cl for H^+ and H_2^+ ions in MeV/amu units. The solid and dashed curves are, respectively, the ECPSSR and PWBAR theories calculated by Lapicki (Ref. 15) and the dotted curves are our extensions. The closed squares are experimental measurements by Maeda *et al.* (Ref. 4) for H^+ ions in gaseous CCl_2F_2. The closed circles and ×, respectively, are the present experimental measurements for H^+ and H_2^+ ions in gaseous CH_3Cl.

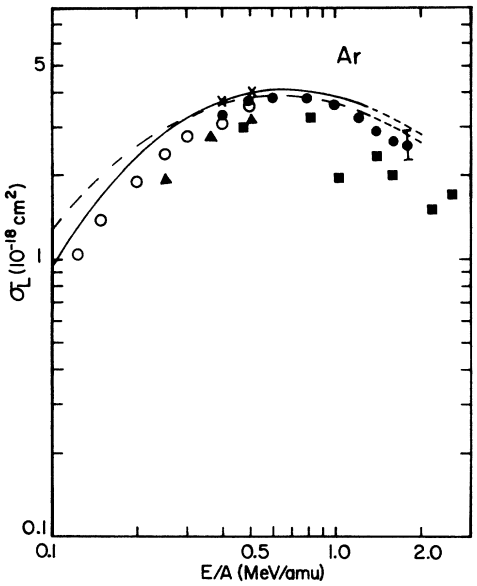

FIG. 6. L-shell-ionization cross sections in 10^{-18} cm^2 in Ar for H^+, H_2^+, and D^+ ions in MeV/amu units. The solid and dashed curves are, respectively, the ECPSSR and PWBAR theories calculated by Lapicki (Ref. 15) and the dotted curves are our extensions. The closed squares are experimental measurements with H^+ ions by Maeda *et al.* (Ref. 4), the solid triangles are experimental measurements with D^+ ions by Watson and Toburen (Ref. 5), the open circles are experimental measurements with H^+ ions by Stolterfoht *et al.* (Ref. 3), the solid circles are present experimental measurements with H^+ ions, and $\times$ are present experimental measurements with H_2^+ ions.

cross sections are scaled according to the BEA prediction of Hansen,[16] all measurements in the region $E_H+/\lambda U_L > 1.5$ are in fair agreement with the theoretical values except for some of the Cl measurements which are as much as 35% higher than the BEA prediction. For $E_H+/\lambda U_L < 1.5$ the experimental values fall below the theory by anywhere from 0% to 31%.

It is explained in Ref. 2 that pure atomic cross sections cannot be obtained from an atom in a molecular environment because of chemical-binding effects which influence the outer electrons in the target atoms within the molecules. These molecular effects were estimated previously[2] for SiH_4, PH_3, and CH_3Cl to be, respectively, 6%, 5%, and 10%. The molecular effect in SO_2 using the same approach in Ref. 2 is estimated to be 16%.

In Fig. 8 an examination of projectile Z_1^2 dependence as a function of the ion energy/amu is given by means of a plot of the L-shell-ionization cross-section ratios $\sigma(He^+)/4\sigma(H^+)$ or $\sigma(He^+)/4\sigma(H_2^+)$ for He^+, H^+, or H_2^+ ions. The $\sigma(He^+)$ cross sections are taken from Ref. 2, while the $\sigma(H^+)$ and $\sigma(H_2^+)$ cross sections are given in Tables I and II. A ratio of unity implies that capture and loss of electrons by the incident ion does not affect the L-shell-ionization cross section which is produced by the nuclear charge of $Z_1=2$ for He and $Z_1=1$ for the proton. The simple Z_1^2 dependence of 4 for He ions and 1 for protons is predicted by the PWBAR and BEA theories, but not for the ECPSSR theory as shown in the figure, where the ratio at low E/A is highest for Si and decreases with Z_2 to Ar. The ECPSSR ratios at $E/A=0.1$ MeV/amu are <1 for S, Cl, and Ar, but >1 for P and Si, and are all ≥ 1 for $E/A \geq 0.2$–1.0 MeV/amu. The experimental ratios from the present L-shell-ionization cross-section measurements from $E/A=0.2$–0.5 MeV/amu are given by the solid points on the figure and are all systematically below unity. A slight trend is revealed that is not inconsistent with the

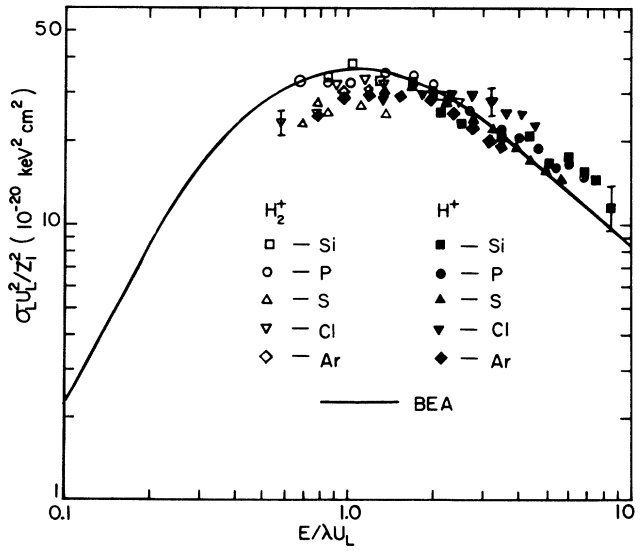

FIG. 7. Experimental L-shell-ionization cross sections of Si, P, S, Cl, and Ar scaled according to the BEA theory. The solid curve represents the BEA prediction by Hansen (Ref. 16).

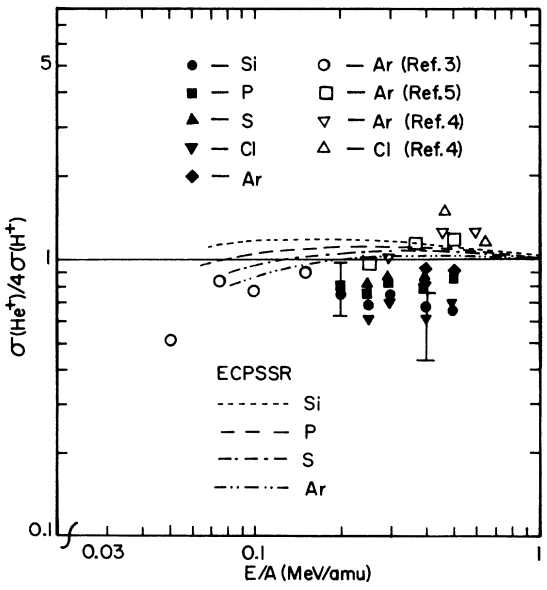

FIG. 8. The ratio of the cross sections produced under He^+ and under H^+, H_2^+, or D^+ ion impact for Si, P, S, Cl, and Ar. The solid symbols represent measurements in this laboratory, while the open symbols are measurements made elsewhere. The ECPSSR theoretical predictions by Lapicki (Ref. 15) are also given for comparison.

qualitative trend of the ECPSSR theory, namely, the P and S ratios are slightly greater than the Cl ratios, but nothing conclusive can be stated because of the large error bars. The open circles,[5] squares,[3] triangles,[4] and inverted triangles[4] represent ratios by other experimental groups for Ar and Cl and follow the ECPSSR trend more closely, although Maeda's Cl measurements for H^+ ions disagree dramatically with the ECPSSR theory, while our Cl measurements agree almost completely with the theory as seen in Fig. 5.

A qualitative description is given which is not inconsistent with the ratios in Fig. 8 produced in this laboratory. In Ref. 2 we stated that the radius of a He^+ ion is 2.65×10^{-11} m, while the Herman and Skillman[18] radius of the Ar L shell is 1.54×10^{-11} m, which yield effective areas of 22.1×10^{-22} and 7.45×10^{-22} m^2 for the He^+ and L shell, respectively. Our statement was that since an energetic 0.6–2.0 MeV He^+ ion was able to penetrate the Ar L shell, and since the He^+ ion's area was about three times that of the Ar L shell, the Ar L shell would see essentially the doubly charged He nucleus so that the Ar L-shell-ionization cross section should be roughly the same for a He^+ ion or He^{2+} ion. The Herman and Skillman L shell radii are 1.64×10^{-11} m (Cl), 1.82×10^{-11} m (S), 1.9×10^{-11} m (P), and 2.1×10^{-11} m (Si), with corresponding areas of 8.45×10^{-22} m^2 (Cl), 10.4×10^{-22} m^2 (S), 11.3×10^{-22} m^2 (P), and 13.8×10^{-22} m^2 (Si). Thus, in going from Ar to Si, the effective area for the L shell to that for the penetrating He^+ ions goes from about 30% to about 62%. This means that the Si L shell is more likely to see the electron on the He^+ ion than is the Ar L shell. An energetic 2-MeV He ion still has about 6% singly charged components and is about 94% doubly charged.[19] If the target-atom L shell sees only $0.94\times2=1.88=Z_1'$ of the doubly charged He ion for ionization purposes, then $Z_1'^2=(1.88)^2=3.53$. Dividing 3.53 by 4 gives 0.88 for the ratio in Fig. 8 for $E/A=0.5$ MeV/amu, and this ratio would decrease further at lower E/A values.[19] Thus, although we are not claiming that our ratios in Fig. 8 are caused by capture and loss of electrons on the He^+ ion passing through the target gases, we are saying that the relative comparable effective areas of the He^+ with those for the L shells for the elements Si, P, S, Cl, and Ar and the fact that a He^+ ion of $E/A=0.2$–0.5 MeV/amu is not fully stripped lend some support to the proposition that this effect should not be completely excluded.

In conclusion, the experimental L-shell-ionization cross sections of Si, P, S, Cl, and Ar measured in this laboratory are found to be from 0% to 37% below the ECPSSR theoretical predictions. Molecular effects, estimated to be from 5% to 16%, and possible anisotropic Auger-electron emission, would lower the L-shell-ionization cross sections even more from the theory.

ACKNOWLEDGMENTS

The authors are grateful to Professor G. Lapicki for providing his ECPSSR and PWBAR calculations that have been used in this paper. We also wish to thank the Baylor University Research Committee and the Department of Physics for their support of the project.

[1]W. Brandt and G. Lapicki, Phys. Rev. A **20**, 465 (1979).
[2]W. M. Ariyasinghe and D. Powers, Phys. Rev. A **41**, 4751 (1990).
[3]N. Stolterfoht, D. Schneider, and P. Ziem, Phys. Rev. A **10**, 81 (1974).
[4]N. Maeda, N. Kobayashi, H. Hori, and M. Sakisaka, J. Phys. Soc. Jpn. **40**, 1430 (1976).
[5]R. L. Watson and L. H. Toburen, Phys. Rev. A **7**, 1853 (1973).
[6]L. H. Toburen, W. E. Wilson, and L. E. Porter, J. Chem. Phys. **67**, 4212 (1978).
[7]D. L. Matthews and F. Hopkins, Phys. Rev. Lett. **40**, 1326 (1978).
[8]S. K. Allison, Rev. Mod. Phys. **30**, 1137 (1958).
[9]S. K. Allison and S. D. Warshaw, Rev. Mod. Phys. **25**, 779 (1953).
[10]L. H. Toburen, Phys. Rev. A **5**, 2482 (1972).
[11]W. M. Ariyasinghe, R. D. McElroy, Jr., and D. Powers, Nucl. Instrum. Methods B **24/25**, 162 (1987).
[12]R. D. McElroy, Jr., W. M. Ariyasinghe, and D. Powers, Phys. Rev. A **36**, 3674 (1987).
[13]B. Cleff and W. Mehlhorn, Phys. Lett. **37A**, 3 (1971).
[14]E. J. McGuire, Phys. Rev. A **3**, 587 (1971).
[15]G. Lapicki (private communication).
[16]J. S. Hansen, Phys. Rev. A **8**, 822 (1973).
[17]G. de Alti and P. Decleva, Chem. Phys. Lett. **45**, 103 (1977).
[18]F. Herman and S. Skillman, *Atomic Structure Calculations* (Prentice-Hall, Englewood Cliffs, NJ, 1963).
[19]J. B. Marion, *Nuclear Data Tables* (National Academy of Sciences—National Research Council, Washington, DC, 1960), Pt. 3, p. 27.